Theoretical Study of Pd(II)- and Ni(II)-Catalyzed Alternating Copolymerization of Carbon Monoxide with Ethylene

Mats Svensson, Toshiaki Matsubara, and Keiji Morokuma*

Cherry L. Emerson Center for Scientific Computation and Department of Chemistry, Emory University, Atlanta, Georgia 30322

Received July 2, 1996[⊗]

The mechanism of the copolymerization of carbonyl with ethylene by model cationic d^8 transition-metal complexes, $(HCNH)_2MMe^+$ (M = Pd, Ni) has been studied. In addition to the hybrid density functional B3LYP method, ab initio MO methods such as MP2, CPF, and PCI-80 have been used as well. In particular, the steps of insertion of carbonyl and ethylene into M−Me and M−COMe bonds have been examined in detail. The activation barriers theoretically determined for the Pd catalyst are compared to recently reported experimental results, and temperature effects are studied for some insertion steps. The Pd-based catalyst is shown to have a better selectivity but a lower reactivity in the alternating copolymerization compared to the Ni analog.

Downloaded by CARLI CONSORTIUM on June 30, 2009
Published on December 24, 1996 on http://pubs.acs.org | doi: 10.1021/om960535u

I. Introduction

Migratory insertion is a fundamental elementary step in organic synthesis and also in catalytic reactions with organometallic compounds.[1] For instance, catalytic olefin polymerization and olefin hydrogenation using transition-metal complexes are widely industrialized processes where olefin migratory insertion plays a key role the reaction. Hydroformylation with a Rh(I) complex, explored by Wilkinson et al. in the 1970s, includes both carbon monoxide insertion and alkene insertion steps in the catalytic cycle.

In addition to many experimental studies, extensive theoretical studies have provided important information concerning the mechanism of migratory insertion, in particular on the transition state (TS) structure, reaction paths, and activation barriers.[2] Using an ab initio molecular orbital (MO) method, Koga and Morokuma have characterized the carbonyl migratory insertion into metal−alkyl and metal−hydrogen bonds for Pd and Pt complexes.[3] They have shown that alkyl and hydride groups actually migrate, stabilizing a three-centered TS via appropriate orbital interaction. Carbonyl insertion into metal−alkyl and metal−hydrogen bonds of $CoR(CO)_4$ and $MnR(CO)_5$ (R = H, CH_3) has been investigated by Versluis and Ziegler with density functional theory (DFT) methods.[4] Berke and Hoffmann studied the orbital interaction for stabilization of the TS for carbonyl insertion into Mn−CH_3 and Mn−H bonds with the extended Hückel method.[5] Nakamura and Dedieu showed the importance of electron correlation for the energetics of carbonyl insertion.[6] Siegbahn et al. have studied the energetics of carbonyl insertion into M−CH_3 and M−H bonds for a sequence of different unsaturated second-row transition-metal complexes using high-quality ab initio methods.[7] The alkene insertion step in the hydrogenation catalytic cycle has also been studied theoretically by many groups. Koga, Daniel, and Morokuma found that C_2H_4 insertion is the rate-determining step in the hydrogenation catalytic cycle using $RhCl(PH_3)_2$ as a model for the Wilkinson catalyst.[8] The insertion of C_2H_4 into the Co−H bond of $CoH(CO)_3$ has been studied by Antolovic and Davidson with ab initio methods and by Versluis et al. with DFT methods.[9] Siegbahn et al. investigated alkene insertion into metal−H and metal−CH_3 bonds for a series of second-row transition-metal atoms with ab initio methods.[10]

Copolymers of carbon monoxide and olefin have attracted much attention from an industrial point of view, because these copolymers have interesting chemical and physical properties.[11] The presence of carbonyl groups in the backbone of the copolymer also makes them easy to modify chemically. Therefore, these copolymers could serve as a good starting material for other classes of functionalized polymers.

The mechanistic aspects of the alternating copolymerization of olefins with carbon monoxide have been thoroughly discussed by Sen.[12] A schematic reaction pathway for the alternating CO/C_2H_4 copolymerization

[⊗] Abstract published in *Advance ACS Abstracts,* November 15, 1996.

(1) Collman, J. P.; Hegedus, L. S.; Norton, J. R.; Finke, R. G. *Principles and Applications of Organotransition Metal Chemistry*; University Science Books: Mill Valley, CA, 1987.
(2) Koga, N.; Morokuma, K. In *Theoretical Aspects of Homogeneous Catalysis*; Leeuwen, P., Morokuma, K., van Lenthe, J., Eds.; Kluwer Academic: Boston, 1995.
(3) (a) Koga, N.; Morokuma, K. *J. Am. Chem. Soc.* **1985**, *107*, 7230. (b) Koga, N.; Morokuma, K. *J. Am. Chem. Soc.* **1986**, *108*, 6136.
(4) Ziegler, T.; Versluis, L.; Tschinke, J. *J. Am. Chem. Soc.* **1986**, *108*, 612.
(5) Berke, H.; Hoffmann, R. *J. Am. Chem. Soc.* **1978**, *100*, 7224.
(6) (a) Nakamura, S.; Dedieu, A. *Chem. Phys. Lett.* **1984**, *111*, 243. (b) Dedieu, A.; Nakamura, S. In *Quantum Chemistry: The Challenge of Transition Metals and Coordination Chemistry*; Veillard, A., Ed., NATO ASI Series 176; Reidel: Dordrecht, The Netherlands, 1986; p 277.
(7) Blomberg, M. R. A.; Karlsson, C.; Siegbahn, P. E. M. *J. Phys. Chem.* **1993**, *97*, 9341.
(8) (a) Koga, N.; Daniel, C.; Han, J.; Fu, X.; Morokuma, K. *J. Am. Chem. Soc.* **1987**, *109*, 3455. (b) Daniel, C.; Koga, N.; Han, J.; Fu, X.; Morokuma, K. *J. Am. Chem. Soc.* **1988**, *110*, 3773.
(9) (a) Antolovic, D.; Davidson, E. *J. Am. Chem. Soc.* **1987**, *109*, 977. (b) Antolovic, D.; Davidson, E. *J. Am. Chem. Soc.* **1987**, *109*, 5828.
(10) (a) Siegbahn, P. E. M. *J. Am. Chem. Soc.* **1993**, *115*, 5803. (b) Siegbahn, P. E. M. *Chem. Phys. Lett.* **1993**, *205*, 290.
(11) (a) Sen, A. *Adv. Polym. Sci.* **1986**, *73/74*, 125. (b) Sen, A. *CHEMTECH* **1986**, 48.
(12) Sen, A. *Acc. Chem. Res.* **1993**, *26*, 303.

S0276-7333(96)00535-3 CCC: $12.00 © 1996 American Chemical Society

Scheme 1. Alternating Copolymerization of C_2H_4 and CO Using a Pd Complex

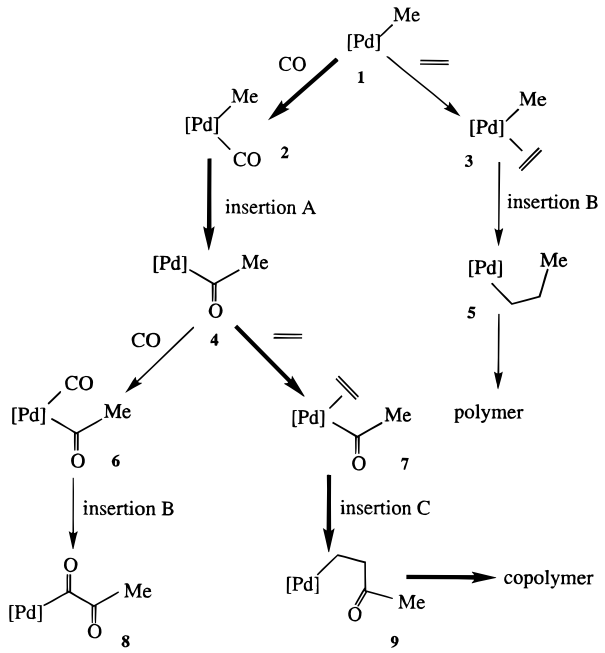

with a Pd complex is presented in Scheme 1. The bold arrows indicate a perfectly alternating CO/C_2H_4 copolymerization reaction pathway. Competing pathways in each insertion step are represented by normal arrows. Brookhart and Rix have recently studied the Pd(II)-mediated perfectly alternating copolymerization of ethylene with carbon monoxide.[13] They successfully compared three kinds of migratory insertion reactions at the same metal center: carbonyl insertion and olefin insertion into a Pd−alkyl bond and the previously unobserved olefin insertion into a Pd−acyl bond, which correspond to migratory insertions A−C, respectively, in Scheme 1. They used the square-planar d^8 Pd(II) complex (1,10-phenanthroline)PdMeL and Ar'_4B^- (L = CO, C_2H_4; Ar′ = 3,5-$(CF_3)_2C_6H_3$) as the starting reactants and isolated several intermediates along the reaction path. Furthermore, they determined the activation free energy barriers $\Delta G^{\ddagger}$ for CO insertion into the Pd−Me bond (insertion A) to be the lowest at 15.4 kcal/mol, followed by 16.6 kcal/mol for C_2H_4 insertion into a Pd-acyl bond (C), 18.5 kcal/mol for C_2H_4 insertion into the Pd−Me bond (B), and 19.4 kcal/mol for CO insertion into the Pd−Et bond, all within errors of 0.1 kcal/mol.

A general advantage of a theoretical approach over an experimental approach is a possibility in theory of determining structures and energies of transition states as well as those of intermediates on the reaction path and investigating the electronic characteristics of the mechanism. Furthermore, ligands and metals can be characterized electronically and sterically independently. In this paper, using a model Pd complex for the Brookhart and Rix system, we optimized all intermediates and transition states included in the reaction pathways presented in Scheme 1 and determined the potential energy surface using a density functional B3LYP method. For the most important parts of the pathways we also performed high-level ab initio calculations. We compared carbonyl and olefin insertion for the same metal complex and clarified the factors which control the different mechanisms. In order to shed light on the mechanism of alternating copolymerization, we also studied corresponding pathways for a Ni complex and compared them with those for the Pd complex.

(13) Rix, C. F.; Brookhart, M. *J. Am. Chem. Soc.* **1995**, *117*, 1137.

II. Methods of Calculation

All calculations were performed using the Gaussian92/DFT package.[14] All transition states as well as equilibrium structures are fully optimized. For Pd complexes they are positively identified as equilibrium geometries (nimag = 0) and transition states (nimag = 1) by the number of imaginary frequencies (nimag) from the analytical Hessian matrix, obtained with our own program for effective core potential (ECP) implemented in the Gaussian package.[15] Structures and vibrational frequencies (and the zero-point energy correction, ZPC) are determined at the density functional B3LYP level, which consists of a hybrid Becke + Hartree−Fock exchange and the Lee−Yang−Parr correlation functional with non-local corrections.[16]

For geometry optimization and frequency calculations, we used basis set I. Basis set I for Pd consists of a (5s5p4d)/[3s3p2d] double-ζ valence basis set with the relativistic ECP developed by Hay and Wadt replacing core electrons up to 3d. For Ni, it is a (5s5p5d)/[3s3p2d] double-ζ valence basis set with the nonrelativistic ECP by Hay and Wadt replacing the 1s, 2s, and 2p core electrons.[17] For carbons, oxygens, and hydrogens of the active parts, i.e. methyl, ethylene, and carbon monoxide, it is the Dunning valence double-ζ basis set,[18] and for carbon, nitrogen, and hydrogen of the inert ligand it is the standard 3-21G basis set. In more accurate single-point calculations a few higher quality basis sets were used. The basis set II is the same as I, except for a triple-ζ valence contraction in the 5s, 5p, and 4d region of the same primitives as in I for Pd, one d polarization function for carbon (0.75) and oxygen (0.85) and one p for hydrogen (1.0) for the active parts, and the Dunning valence double-ζ basis set for the inert ligand. When the polarization functions were added to basis set I, it was labeled as I+P. In some cases one f polarization function was added to basis set II on Pd,[19] giving basis set II+f.

We performed some coupled-pair functional (CPF)[20] calculations for selected intermediates using basis set III. For carbons, nitrogens, oxygens, and hydrogens the basis set III is identical with II. The basis set III for Pd is a (17s13p9d3f)/[7s6p4d1f] set, with the Huzinaga primitive basis set[21] augmented by two diffuse p, one diffuse d, and three f functions and with the full contraction for core, a double-ζ contraction for 4s and 4p, a triple-ζ contraction for 5s and 5p orbitals, and a full contraction for f.[22] Relativistic effects in the calculations using this basis set were accounted for using first-order perturbation theory, including the mass−velocity and Darwin

(14) Gaussian 92/DFT, Revision F.2: M. J. Frisch, G. W. Trucks, H. B. Schlegel, P. M. W. Gill, B. G. Johnson, M. W. Wong, J. B. Foresman, M. A. Robb, M. Head-Gordon, E. S. Replogle, R. Gomperts, J. L. Andres, K. Raghavachari, J. S. Binkley, C. Gonzalez, R. L. Martin, D. J. Fox, D. J. Defrees, J. Baker, J. J. P. Stewart, and J. A. Pople, Gaussian, Inc., Pittsburgh, PA, 1993.

(15) Cui, Q.; Musaev, D.; Svensson, M.; Morokuma, K. *J. Phys. Chem.* **1996**, *100*, 10936.

(16) Becke, A. D. *J. Chem. Phys.* **1993**, *98*, 5648.

(17) Hay, P.; Wadt, W. *J. Chem. Phys.* **1985**, *82*, 299.

(18) Dunning, T.; Hay, P. In *Modern Theoretical Chemistry*; Ed. Schaefer, H., III, Ed.; Plenum: New York, 1976; p 1.

(19) Ehlers A. W.; Böhme, M.; Dapprich, S.; Gobbi, A.; Höllwarth, A.; Jonas, V.; Köhler, K. F.; Stegmann, R.; Veldkamp, A.; Frenking, G. *Chem. Phys. Lett.* **1993**, *208*, 111.

(20) Ahlrichs, R.; Scharf, P.; Ehrhardt, C. *J. Chem. Phys.* **1985**, *82*, 890.

(21) Huzinaga, S. *J. Chem. Phys.* **1965**, *42*, 1293.

(22) (a) Almlöf, J.; Taylor, P. R. J. *Chem. Phys.* **1987**, *86*, 4070. (b) Raffinetti, R. C. *J. Chem. Phys.* **1973**, *58*, 4452.

Downloaded by CARLI CONSORTIUM on June 30, 2009
Published on December 24, 1996 on http://pubs.acs.org | doi: 10.1021/om960535u

terms.[23] As recently presented by Siegbahn et al., the tendency of methods such as CPF and CCSD to underestimate correlation effects can effectively be accounted for by scaling the correlation energy. The scheme proposed is called PCI-80,[24] where 80 indicates that the calculated correlation energy is scaled by 1/0.80. For a selected number of important intermediates PCI-80 relative energies will also be reported.

III. Structures and Energies of Intermediates and Transition States

All intermediates and transition states shown in Scheme 1 are fully optimized at the B3LYP/I level. In order to save computational time, we adopted ethanediimine, NH=CHCH=NH, as a model for 1,10-phenanthroline (phen) used as a ligand in the experiment and we will refer to it as phen′. We also used *N*,*N*′-dimethylethanediimine, referred to as phen″, in order to evaluate some steric and electronic effects which could be important for the insertion steps.

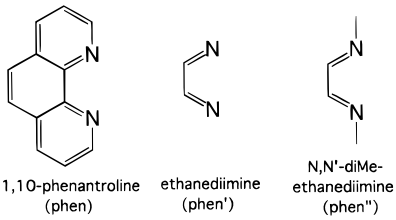

In this section, we will begin our discussion with the coordination of CO and C_2H_4 to the methyl complex (phen′)MMe$^+$ (**1**) for M = Pd and Ni. We will then examine the transition states and products of the migratory insertion step. Then we will discuss CO and C_2H_4 coordination to the acyl complex, followed by the transition states and products of insertion.

A. CO and C_2H_4 Coordination to Alkyl Complexes. The B3LYP/I-optimized structures of the reactants, i.e. the methyl complex (phen′)PdMe$^+$ (**1**) and free CO and C_2H_4, as well as of the CO and C_2H_4 coordination complexes, (phen′)Pd(CO)Me$^+$ (**2**) and (phen′)Pd(C_2H_4)Me$^+$ (**3a,b**), are shown in Figure 1. For Ni, structures of only **1**, **2**, and **3b** were optimized and their geometrical parameters are shown in parentheses. The B3LYP/I energies of these species, relative to the reactant **1** and an appropriate number of free CO and C_2H_4 molecules, are given in Table 1 for both Pd (with and without ZPC) and Ni (without ZPC).

The reactant (phen′)PdMe$^+$ (**1**), an unsaturated 14-electron complex, has a C_s symmetry. The principal axis of its methyl ligand is coplanar with the phen′ ligand and is trans to one of the nitrogen atoms, leaving an empty site trans to the other nitrogen. As expected for a 16-electron Pd(II) complex, the carbonyl complex (phen′)Pd(CO)Me$^+$ (**2**), also with C_s symmetry, has a square-planar structure in which CO is head-on and cis to the methyl ligand. The CO ligand, as well as the ethylene ligand, interacts with Pd through σ-donation and π-back-donation, as described by the Dewar−Chatt−Duncanson model. For ethylene complex (phen′)-Pd(C_2H_4)Me$^+$ (**3**), the two equilibrium structures (nimag = 0) **3a** and **3b** exist, where the C=C bond of ethylene is either coplanar with the phen′ plane in **3a** or perpendicular in **3b**. A very small barrier for rotation exists between **3a** and **3b** but will not be discussed here. Ethylene is more strongly bound to the metal in **3b** than in **3a**; the C=C bond distance is 0.01 Å longer and the Pd−ethylene X (the midpoint of the C=C bond) distance is 0.10 Å shorter in **3b** than in **3a**. This is understood by the fact that in **3b** the dπ orbital of the metal can back-donate electrons to the π* orbital of ethylene. As a consequence of the stronger olefin interaction in **3b**, the trans Pd−N bond in **3b** is 0.03 Å longer than in **3a**. The Pd−N distance in **3b** is almost the same as in carbonyl complex **2**, indicating that here the trans influence of ethylene with back-donation is similar to that of CO. In structure **3a**, the methyl−Pd−X angle is 3° larger than in **3b**, due to a larger steric repulsion between methyl and ethylene. Complex **3b** is 5 kcal/mol more stable than **3a**.

For Ni, all structures are qualitatively similar to those of Pd. The smaller covalent radius of the Ni atom makes all the bond lengths to the metal approximately 0.12 Å shorter. The C−C bond in **3b** is slightly less activated, i.e., 0.01 Å shorter, for Ni than for Pd. The methyl−Ni−X angle is 2° larger than that for Pd, presumably due to greater methyl−ethylene steric repulsion in the more compact Ni complex.

The binding energy of CO in carbonyl complex **2**, 41.1 kcal/mol (38.5 kcal/mol with ZPC), is 9 kcal/mol larger than the binding energy 31.7 kcal/mol (29.4 kcal/mol with ZPC) of C_2H_4 in olefin complex **3b** for Pd at the present level of theory. As pointed out by Sen,[12] the π-complexation energy of CO is generally larger than that of C_2H_4 due to the greater π-acidity of CO. The d^8 Pd atom back-donates electrons into two more electronegative empty π* orbitals on CO, but only into one less electronegative π* on C_2H_4. The binding energies of 39.6 kcal/mol for CO and 27.9 kcal/mol for C_2H_4 in Ni complexes are a few kilocalories per mole smaller than those in Pd.

B. Transition States and Products of Carbonyl and Olefin Insertion at the Alkyl Complex. The optimized transition state structure **TS(2−4a)** with C_s symmetry for the intramolecular migratory insertion of CO in Pd(phen′)(Me)(CO) (**2**) is also shown in Figure 1. The reaction coordinate, shown in Figure 2, demonstrates clearly that it is the methyl group, not the carbonyl group, that migrates during the reaction and that the reaction leads to the product **4a** maintaining the C_s symmetry, as shown in Figure 2. The situation is similar to that found by Koga et al. for Pd(PH_3)(Me)-(CO).[3]

In **TS(2−4a)** the Pd−C bond is shorter (1.87 Å) than in the reactant **2** (1.92 Å) or in the insertion product **4** (1.95 Å). In the transition state, the out-of-plane π-donation from Pd into the π*-orbital on CO is still present when the Pd−C σ-bond is starting to be formed. **TS(2−4a)** is considered to be an early and tight TS, as the breaking Pd−CH_3 bond is only 0.23 Å longer than in the reactant **2** and the forming CH_3−CO bond is still 0.36 Å longer than in the product **4a**. **TS(2−4a)** for Ni is tighter than for Pd, reflecting the smaller size of the metal.

The geometries of the insertion products, the 14-electron Pd−acyl complexes **4a** and **4b**, are given in Figure 1. Complex **4a** is the direct product of the

(23) Martin, R. L. *J. Phys. Chem.* **1983**, *87*, 750.
(24) (a) Siegbahn, P. E. M.; Blomberg, M. R. A.; Svensson, M. *Chem. Phys. Lett.* **1994**, *223*, 35. (b) Siegbahn, P. E. M.; Svensson, M.; Boussard, P. J. E. *J. Chem. Phys.* **1995**, *102*, 5377.

Downloaded by CARLI CONSORTIUM on June 30, 2009
Published on December 24, 1996 on http://pubs.acs.org | doi: 10.1021/om960535u

Downloaded by CARLI CONSORTIUM on June 30, 2009
Published on December 24, 1996 on http://pubs.acs.org | doi: 10.1021/om960535u

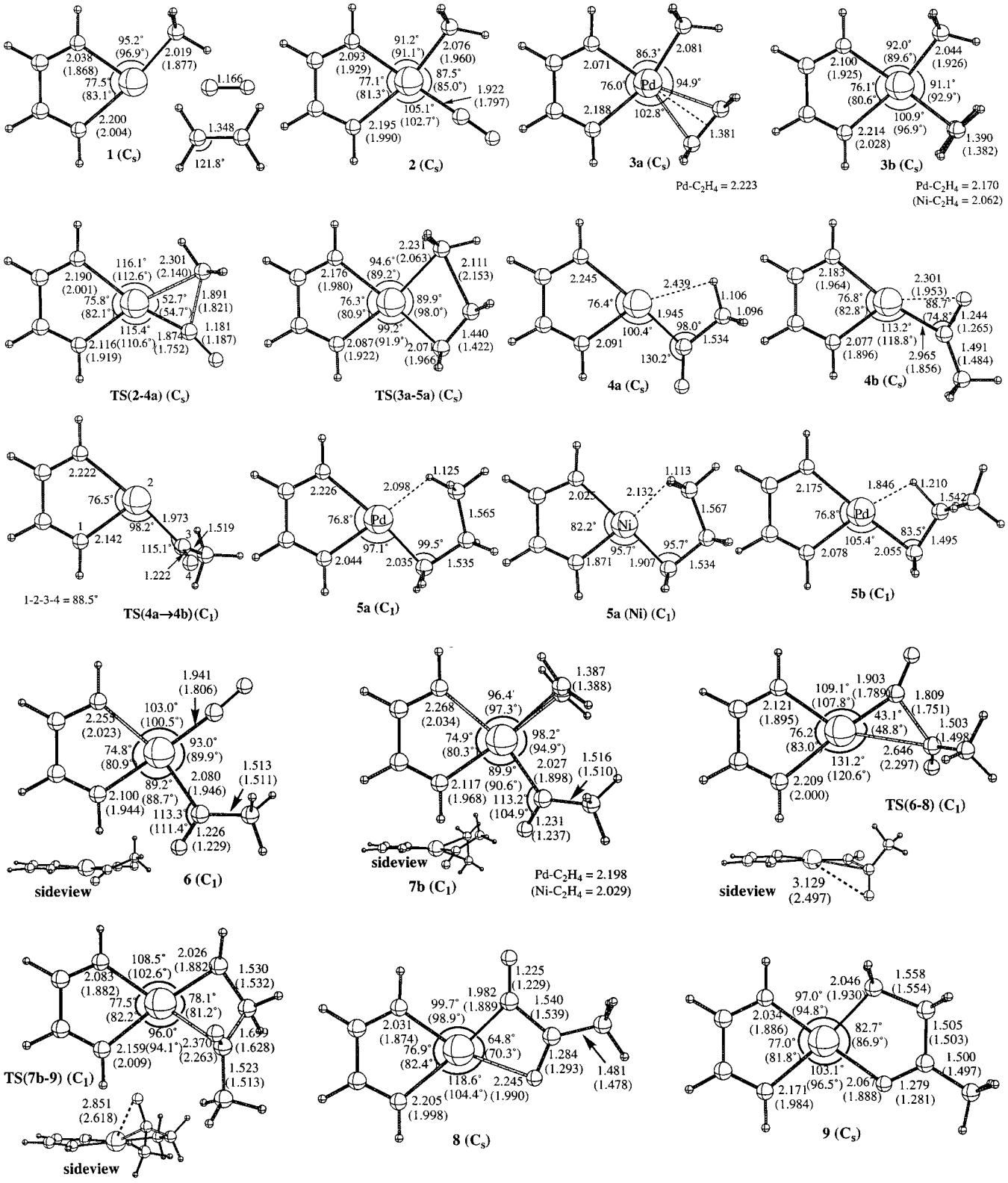

Figure 1. B3LYP/I optimized structures (in Å and deg) of intermediates and transition states for the ethylene/CO copolymerization reactions of Scheme 1. Numbers without parentheses are for Pd; those in parentheses are for Ni. For Pd, each structure has been characterized by the Hessian analysis as an intermediate (nimag = 0) and transition state (nimag = 1). The M−C_2H_4 distance in the figure is the distance between M and the center X of the C═C bond of C_2H_4.

migratory insertion. Complex **4b** is reached after 180° rotation along the Pd−C bond via the transition state **TS(4a−4b)**. Both **4a** and **4b** are planar C_s structures, while in **TS(4a−4b)** the carbonyl group is rotated 88.5° out of the plane. In **4a**, a weak agostic interaction is seen between a hydrogen on the methyl group and Pd, with a Pd−C−C angle of 98.0°, a Pd−H distance of 2.44 Å, and a C−H distance longer by 0.010 Å than the normal 1.096 Å. The interaction is weak because the carbonyl group adjacent to the CH_3 group reduces its donating capacity. In **4b**, a substantial chelative interaction between the carbonyl oxygen and the Pd center is present, as seen from the small Pd−C−O angle of 88.7° and the short Pd−O distance of 2.30 Å. The

Table 1. B3LYP/I Energies (in kcal/mol), Relative to (phen′)MMe$^+$ (1; M = Pd, Ni) and an Appropriate Number of Free CO and C_2H_4 Molecules, for the Intermediates and Transition States for Copolymerization of Carbon Monoxide and Ethylene

	Pd		Ni
structure	ΔE	ΔE + ZPC[a]	ΔE
1	0.0	0.0	0.0
2	−41.1	−38.5	−39.6
3a	−26.8	−24.5	
3b	−31.7	−29.4	−27.9
TS(2−4a)	−26.1	−23.8	−29.8
TS(3a−5a)	−15.5	−12.8	−18.0
4a	−32.7	−29.6	
4b	−39.1	−35.4	−45.2
TS(4a−4b)	−29.5		
5a	−31.8	−27.8	−33.3
5b	−37.4	−33.9	−39.4
6	−67.4	−61.8	−64.6
7b	−58.2	−52.8	−52.8
TS(6−8)	−39.2	−34.3	−39.7
TS(7b−9)	−40.0	−34.7	−46.5
8	−51.9	−45.3	−57.5
9	−80.5	−72.9	−87.9

[a] ZPC is the zero-point correction calculated at the B3LYP/I level.

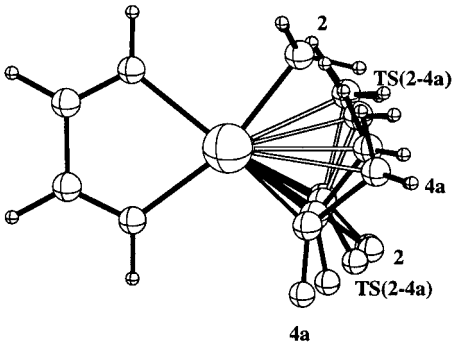

Figure 2. Geometries of the carbonyl insertion reactant **2**, the transition state **TS(2−4a)**, IRC points between this TS and **4a**, and the product **4a** for the (phen′)PdMe complex, superimposed while keeping the maximum overlap of the Pd−(NCCN) fragment. Migration of the methyl group is clearly seen.

carbonyl oxygen coordinates more strongly for the more compact Ni (**4b**), as seen from the smaller Ni−C−O angle of 74.8° and the notably shorter Ni−O distance of 1.95 Å.

Complex **4b** for Pd with the chelating oxygen is 6.4 kcal/mol (5.8 kcal/mol ZPC) more stable than **4a** with the agostic hydrogen. **4a** rearranges into **4b** with a 4.8 kcal/mol activation barrier at **TS(4a−4b)**. The overall exothermicity for the reaction **1** + C_2H_4 → **4b** is 6.1 kcal/mol larger for Ni as a result of the stronger metal−oxygen coordination.

The transition state for ethylene insertion, **TS(3a−5a)**, is planar. From the most stable ethylene complex, **3b**, ethylene has to rotate first by 90° to form complex **3a**, before the insertion can begin. Though the barrier for this rotation has not been studied here, it is expected to be low. **TS(3a−5a)** can be classified as an earlier transition state than **TS(2−4a)**. The breaking Pd−Me bond is 0.07 Å shorter in **TS(3a−5a)** than in **TS(a−4a)** and the forming C−C bond is longer by 0.22 Å in **TS(3a−5a)** than in **TS(2−4a)**.

A notable difference in transition states between CO and C_2H_4 insertions is that in the ethylene insertion **TS(3a−5a)** the Pd−C distance is longer than in the product **5a**, whereas in the carbonyl insertion **TS(2−4a)** it is shorter than in the product **4a**. This could be attributed to the existence of an out-of-plane π*-orbital for CO insertion and the lack of it for C_2H_4 insertion.

Two optimized structures are found for the ethylene insertion product (phen′)Pd($CH_2CH_2CH_3$)$^+$ (**5**). Complex **5a** with a γ-agostic interaction can be considered as the direct product of olefin insertion from the olefin complex **3a** via **TS(3a−5a)**. The strong γ-agostic interaction elongates the C−H bond by 0.03 Å from the normal C−H distance of 1.09 Å, with a relatively short Pd−H distance of 2.10 Å. Complex **5a** rearranges to the more stable β-agostic complex **5b**, with a very long C−H bond of 1.21 Å and a short Pd−H distance of 1.85 Å. The Ni complex corresponding to **5a** is shown separately in Figure 1, where Ni prefers to interact with two γ-hydrogen atoms, rather than one in the Pd species **5a**. These C−H bonds are less stretched and the M−H distances are longer than in the Pd analog. For both Pd and Ni, **5b** is more stable than **5a** by about 6 kcal/mol, with or without ZPC.

C. CO and C_2H_4 Coordination to Acyl Complexes. Now we consider coordination of CO and C_2H_4 to the acyl complex (phen′)Pd($COCH_3$)$^+$ (**4**), which results in (phen′)Pd(CO)($COCH_3$)$^+$ (**6**) and (phen′)Pd(C_2H_4)($COCH_3$)$^+$ (**7**), respectively, as shown in Figure 1. For **7**, we only optimized the geometry **7b** with the C═C bond perpendicular to the N−M−N plane.

If we compare **6** and **7b** with **2** and **3b**, respectively, we find that both the Pd−CO and Pd−C_2H_4 bond distances in the acyl complexes are 0.01−0.02 Å longer than in the alkyl complexes. The carbonyl group is rotated out from the N−Pd−N plane by 26.9° in **6** and by 39.4° in **7b**, presumably due to the steric repulsion between the carbonylic oxygen and the phen′ ligand. This increased steric repulsion is also illustrated by the somewhat smaller N−Pd−N bite angle in **6** relative to **2**. The orientation of the acyl group in **6** and **7b** corresponds to that in complex **4a**, but due to the presence of CO and C_2H_4 ligands, respectively, the agostic interaction present in **4a** is broken and the methyl group is bent away from these ligands to avoid the repulsion.

Due to the smaller metal size, Ni complexes **6** and **7b** have their carbonyl group rotated out of the N−Ni−N plane substantially more, i.e. 60.7 and 73.7°, respectively. In the real system with 1,10-phenanthroline, instead of the phen′ model, this repulsion would be larger and the carbonyl group would probably be rotated as much as 90° out of the N−M−N plane. In carbonyl complex **6**, all four coordinating ligands are coplanar within 1°. In **7b**, the C_2H_4 group does not coordinate in the plane; the midpoint of the olefin is rotated 20.0° out of the N−Ni−N plane and the carbonylic carbon is at the same time rotated 11.2° in the opposite direction out of the plane, presumably to avoid the greater repulsion. The square planarity of this Ni(II) olefin complex is thereby starting to be less well-defined. This somewhat surprising result is most likely related to that it is starting to be crowded in the plane for the small Ni atom and that, in addition, a substantial part of the C_2H_4 interaction with this cationic complex is electrostatic and does not require an in-plane coordination.

For Pd, the CO complex **6** is about 10 kcal/mol more

Downloaded by CARLI CONSORTIUM on June 30, 2009
Published on December 24, 1996 on http://pubs.acs.org | doi: 10.1021/om960535u

Downloaded by CARLI CONSORTIUM on June 30, 2009
Published on December 24, 1996 on http://pubs.acs.org | doi: 10.1021/om960535u

stable than the C_2H_4 complex **7b**; the situation is similar for the comparison between **2** and **3b**. However, the absolute π-complexation energies of CO and C_2H_4 to acyl complex **4b**, 28.3 kcal/mol and 19.1 kcal/mol, respectively, are about 13 kcal/mol less than those to the alkyl complex **1**. This is because the strong Pd−O chelating interaction in the unsaturated 14-electron Pd(phen′)Ac complex has to be broken before CO or C_2H_4 can coordinate, therefore reducing the complexation energy. For Ni the π-complexation energy of CO is 19.4 kcal/mol and for C_2H_4 7.6 kcal/mol. Again the difference seen between carbonyl and olefin binding energies is the same as for the metal−alkyl complex. These small complexation energies are related to the stronger Ni−O bond in **4b** that has to be broken before CO or C_2H_4 can coordinate.

D. Transition States and Products of Carbonyl and Olefin Insertion at the Acyl Complex. The transition state for CO insertion, **TS(6−8)**, into the Pd−acyl bond is shown in Figure 1. It should be noticed that the acyl group is rotated out-of-plane by 61.3°, 34.4° more than in reactant **6**. The Pd−O distance is 3.13 Å in **TS(6−8)**, which is too long for an energetically important interaction. It is interesting to compare the CO insertion into the Pd−Ac bond in **TS(6−8)** with the CO insertion into the Pd−Me bond in **TS(2−4a)**. The acyl group migrates in **TS(6−8)** as the alkyl group migrates in **TS(2−4a)**. **TS(6−8)** is a later TS than **TS-(2−4a)**, as seen from the shorter C−C bond of 1.81 Å in the former vs 1.89 Å in the latter. The C−Pd−C angle is 10° smaller in **TS(6−8)**, which makes this TS much more strained than **TS(2−4a)**.

For Ni, **TS(6−8)** is less strained than for Pd, as seen from the C−Ni−C angle, which is 6° larger. The C−C bond is 0.06 Å shorter for Ni as well. The acyl group is closer to the metal for Ni than for Pd; for instance, the M−O distance is 2.50 Å for Ni vs 3.13 Å for Pd. The M−O interaction out of the N−M−N plane is repulsive, because the lone pair on oxygen interacts repulsively with filled d orbitals on the metal. For Ni the d shell is more compact, making this repulsion smaller, and therefore the carbon on the acyl group can be closer to the metal. This is in line with the 0.35 Å shorter $M-C_{acyl}$ distance for Ni compared to Pd.

The activation barrier for the migratory insertion of CO into the M−Ac bonds is clearly larger than for the insertion into the M−Me bonds. The difference is 13−14 kcal/mol for both Pd and Ni. This is related to the low stability of the product from the insertion into the M−Ac bond, as will be discussed below. In a comparison of CO insertion between Ni and Pd, the activation barrier for Ni is lower than for Pd. In **TS(6−8)** this difference is 3 kcal/mol and this is somewhat smaller than 6 kcal/mol in **TS(2−4a)**.

In the CO insertion product **8**, the oxygen of the β-carbonyl interacts with the Pd atom at the available empty site and a planar four-membered chelated complex is formed, with a Pd−O length of 2.24 Å. The Pd−O interaction is not ideal, as seen from the small C−Pd−O angle of 64.8°, compared to the normal square-planar angle of 90°. The C−O bond for the chelating CO group is stretched to 1.28 Å, as compared to 1.22 Å for the noncoordinating CO group. This is longer than the 1.24 Å in the three-membered complex **4b**, where the Pd−O interaction is even more strained. For Ni the four-membered insertion product has even stronger chelation, as seen from the more stretched C−O bond, the C−M−O angle, which is 5° larger, and the Ni−O bond, which is 0.25 Å shorter than in the Pd analog.

The endothermicity of the rearrangement reaction **6** → **8** is 15.5 kcal/mol for Pd and 7.1 kcal/mol for Ni. In contrast, the rearrangement **2** → **4a** was only 2.0 kcal/mol endothermic for Pd and 5.6 kcal/mol exothermic for Ni. The main reason behind a smaller driving force for insertion into the M−Ac bond, compared to insertion into the M−Me bond, exists in the difference in the reaction energies without metal. The exothermicities of the reactions CO + Me → COMe and CO + COMe → COCOMe are calculated to be 25.4 and 10.0 kcal/mol, respectively, at the present B3LYP/I level. Most of the 13 kcal/mol difference in the driving force in the metal-catalyzed reactions, seen for both Pd and Ni, comes from that of the corresponding reactions without a catalyst.

The transition state **TS(7b−9)** for ethylene insertion into the Pd−Ac bond of **7** is shown in Figure 1. The acyl oxygen is rotated out of the N−Pd−N plane more than in reactant **7**. In **TS(7b−9)**, the $Pd-C_{acyl}$ bond is stretched by 0.34 Å and the C−C double bond becomes a single bond of 1.53 Å, indicating that **TS(7b−9)** is a late TS. This can be compared with the earlier **TS(3a−5)** for ethylene insertion into the Pd−Me bond, where some double-bond character still remains, as seen from the C−C distance of 1.44 Å. The forming C−C bond of 1.70 Å in **TS(7b−9)** is much shorter than the 2.11 Å in **TS(3a−5)**, in agreement with the characterization of **TS(7b−9)** as a later TS than **TS(3a−5)**. **TS(7b−9)** for Ni is similar to that for Pd. The double bond became again a single bond, and the forming C−C bond is even shorter (1.63 Å) for Ni.

The activation barrier for ethylene insertion into the Pd−Ac bond is 18.2 kcal/mol, which is in the same range as the insertion into the Pd−Me bond (16.2 kcal/mol). For Ni both activation barriers are lower compared to Pd; especially the barrier for insertion into the Ni−Ac bond, 6.3 kcal/mol, is almost 12 kcal/mol lower than for Pd. The large exothermicity in the insertion steps, together with the smaller repulsion between the carbonyl oxygen and the valence d shell for Ni, is responsible for these results.

In Figure 1 the structure of ethylene insertion product **9** into the Pd−Ac bond of **7b** is shown. This is a five-membered ring where the acyl oxygen interacts strongly with the Pd metal center. The Pd−O bond is 2.07 Å, and the C−O bond is elongated to 1.28 Å. This chelating structure is less strained than complex **8**, as seen from the C−Pd−O angle of 82.7° vs 64.8° in the latter. The product of ethylene insertion into the Pd−Me bond, **5a**, can also be classified as a five-membered ring. In this agostic structure the γ-hydrogen interacts with the empty site of the Pd complex, just as the oxygen in **9**. In both cases an internal rotation around the CC bond must take place to create an empty site before the next olefin or CO can coordinate. This step has not been studied here though. The insertion product **9** is a five-membered chelating structure for Ni as well. The Ni−O bond is 0.18 Å shorter than the Pd−O bond. Ni, as compared with Pd, does not like agostic interaction as much as the interaction with a strongly donating oxygen. The C−O bond in **9** for Ni is as long as for Pd

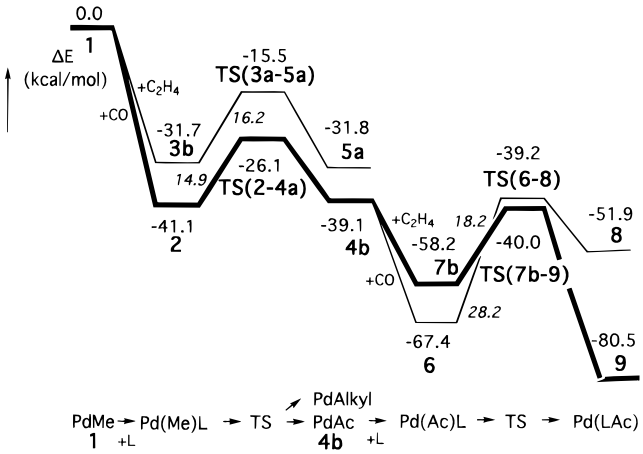

Figure 3. Potential energy profile of ethylene/CO copolymerization reaction steps for (phen′)PdMe as the starting catalyst. The energy is at the B3LYP/I level without ZPC, for comparison with Figure 4.

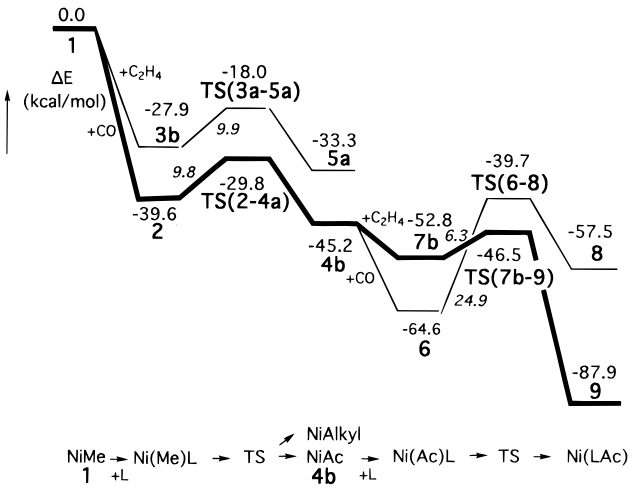

Figure 4. Potential energy profile of ethylene/CO copolymerization reaction steps for (phen′)NiMe as the starting catalyst. The energy is at the B3LYP/I level without ZPC.

(1.28 Å), but the agostic C−H bond in **5a** is shorter for Ni than for Pd.

The exothermicity of the reaction **1** + C_2H_4 + CO → **9** is 80.5 kcal/mol for Pd and 87.9 kcal/mol (7.4 kcal/mol larger) for Ni. The difference in exothermicity between Ni and Pd for the reaction **1** + C_2H_4 → **5a** is smaller: 1.5 kcal/mol more exothermic with Ni. This is in line with the geometry observations above that Ni prefers to interact with the oxygen in **9** over the an agostic hydrogen in **5a**.

IV. Overall Potential Energy Surfaces of Copolymerization

With the alkyl complex **1** as the starting point, there are two reaction paths. One is ethylene insertion, indicated by a normal line, and the other is carbonyl insertion, indicated by a bold line in Scheme 1. For the second insertion reaction starting from the acyl complex **4**, two reaction paths exist as well. For a perfectly alternating copolymer of CO and C_2H_4, the CO/C_2H_4 selectivity in each insertion step is very critical. We will begin to discuss the insertion reactions from the alkyl complex **1** in the next subsection, where a test of the computational accuracy constitutes a significant part. After discussion on the insertion reactions at the acyl complex **4a**, the entire potential energy surface will be summarized and conclusions concerning the mechanism of alternating copolymerization will be made. The B3LYP/I potential energy surfaces connecting the reactants, intermediates, and transition states for copolymerization are presented in Figure 3 for Pd and in Figure 4 for Ni.

A. Insertion Reactions at the Alkyl Complex. As presented in Figure 3, the reaction barrier for the carbonyl insertion and the ethylene insertion is 14.9 and 16.2 kcal/mol, respectively, at the B3LYP/I level for Pd. These results indicate that carbonyl insertion into the Pd−Me bond kinetically is more favorable than ethylene insertion, in agreement with experimental results. The experimental difference was measured to be 3.1 kcal/mol, as compared to 1.3 kcal/mol at the B3LYP/I level. In order to test our computational accuracy, we calculated the activation barriers improving the basis sets at the B3LYP level and using various ab initio methods, as shown in Table 2. To allow a direct comparison with the experimental activation free energy $\Delta G^{\ddagger}$, we included in Table 2 the enthalpy and entropy effects at the experimental temperatures (−66 °C for CO insertion and −25 °C for C_2H_4 insertion) calculated at the B3LYP/I level. The thermal effects decreased the CO insertion barrier by 0.2 kcal/mol and increased the C_2H_4 insertion barrier by 1.1 kcal/mol.

Within the B3LYP approximation, going from basis set I to basis set II, i.e. from double-ζ to triple-ζ basis + polarization functions (on active atoms), does not change the activation barriers more than 0.3 kcal/mol. The absolute difference to the experimental determined activation barriers does not exceed 0.9 kcal/mol at the B3LYP/II+f level and 1.2 kcal/mol at the B3LYP/I level. All ab initio methods, on the other hand, appear to overestimate the CO insertion barrier by 3−4 kcal/mol, resulting in a very small or no kinetic preference for CO insertion, opposite to the results of experiment and B3LYP.

The reason for this behavior can be related to modeling the experimental 1,10-phenanthroline (phen) by ethanediimine (phen′). We therefore calculated the activation barriers using the somewhat larger *N*,*N*-dimethylethanediimine (phen″ in Scheme 1). At the B3LYP/I level, the CO insertion barrier decreases 0.7 kcal/mol while the C_2H_4 insertion barrier increases 0.7 kcal/mol. Thus, the difference in the activation barriers of CO and C_2H_4 insertion is changed by 1.4 kcal/mol when phen′ is replaced by phen″. Adding this effect, the kinetic preference for CO insertion versus C_2H_4 insertion is qualitatively correct, compared to experiment, at all theoretical levels.

All the activation barriers for the Ni complexes shown in Figure 4 are 5−6 kcal/mol lower than those for Pd shown in Figure 3. The difference between the CO and C_2H_4 activation energies is reduced to 0.1 kcal/mol from 1.3 kcal/mol for Pd. In the last part of this section the difference between Pd and Ni will be discussed more in detail.

B. Insertion Reactions at the Acyl Complex. As seen in Figure 3, for the CO/C_2H_4 insertion into the Pd−acyl bond of Pd(phen′)$(COMe)^+$ (**4b**) the barrier for olefin insertion, 18.2 kcal/mol, is lower than that for carbonyl insertion, 28.2 kcal/mol. An experimental activation barrier, 16.6 kcal/mol, is reported only for the olefin

Downloaded by CARLI CONSORTIUM on June 30, 2009
Published on December 24, 1996 on http://pubs.acs.org | doi: 10.1021/om960535u

Table 2. Activation Free Energies (in kcal/mol) for CO and C_2H_4 Insertion into the Pd−Me Bond Using Different Methods and Basis Sets, at the B3LYP/I Optimized Geometries[a]

	phen′							phen″	
	B3LYP				MP2	CPF	PCI-80	B3LYP	phen
method	I	I+P	II	II+f	II+f	III	III	I	exptl
CO	14.7	14.4	14.9	14.9	17.8	18.9	17.6	14.0	15.4
C_2H_4	17.3	16.1	17.7	17.6	18.4	18.7	17.9	18.0	18.5
Δ(CO−C_2H_4)	+2.6	+1.7	+2.8	+2.7	+0.6	−0.2	+0.3	+4.0	+3.1

[a] The thermal (enthalpy and entropy) contribution calculated at the B3LYP/I level is included at −66 °C for CO insertion and at −25 °C for C_2H_4 insertion.

insertion, which compares well with the calculated value of 18.2 kcal/mol. For the olefin insertion, the interaction of oxygen on the acyl group with the Pd metal center stabilizes this transition state, compared to that in the CO insertion, as seen in the less strained C−Pd−C angle in **TS(7b−9)**; 78.1° compared to 43.1° in **TS(6−8)**.

The insertions of CO and C_2H_4 into the Ni−Ac bond both have lower activation barriers than for the Pd system. If one compares the energy at the CO insertion transition state relative to the reactant complex **1**, they are very similar: −39.2 kcal/mol for Pd and −39.7 kcal/mol for Ni. The lower activation barrier for the CO insertion for Ni, 24.9 kcal/mol, can be attributed to the lower stability of π-complex **6** for Ni. Using the same argument for the C_2H_4 insertion, the very low activation barrier for Ni of 6.3 kcal/mol, compared to 18.2 kcal/mol for Pd, is a result of the higher energy of π-complex **7b**, −52.8 kcal/mol for Ni versus −58.2 kcal/mol for Pd, together with the lower energy of **TS(7b−9)**, −46.5 kcal/mol for Ni versus −40.0 kcal/mol for Pd.

As mentioned above, the Pd(phen′)$(COMe)^+$ complex binds CO 9 kcal/mol stronger than C_2H_4 and the CO insertion into the Pd−Me bond is favored over the olefin insertion. However, the CO insertion into a metal−acyl bond is endothermic by 15.5 kcal/mol for Pd and 7.1 kcal/mol for Ni. The barrier for CO insertion is high: 28.2 kcal/mol for Pd and 24.9 kcal/mol for Ni. This means that homopolymerization of carbon monoxide will not take place. Experimentally, no activation barrier has been reported for CO insertion into the M−acyl bond. In contrast, the C_2H_4 insertion step is exothermic by 22.4 kcal/mol for Pd and 35.1 kcal/mol for Ni, which partially is a consequence of the stronger coordination of the carbonylic oxygen atom to the M center for **9**. Both complexes **8** and **9** are found to have planar structures. The strong carbonyl coordination to the metal center forces the planarity, despite some strain energy in the cyclic structures. The C−Pd−C angle of 82.7° in **9** is smaller than 64.8° in **8** and is much closer to the ideal angle of 90° for best overlap.

C. Alternating Copolymerization. Putting all the results together, we will finally discuss the entire potential energy surface of the alternating copolymerization reaction. For Pd, the order of the activation energies at the B3LYP/I level for the migratory insertion reactions (in kcal/mol) is: $\Delta E_{Me\rightarrow CO} = 14.9 < \Delta E_{Me\rightarrow C_2H_4} = 16.2 < \Delta E_{Ac\rightarrow C_2H_4} = 18.2 < \Delta E_{Ac\rightarrow CO} = 28.2$. The corresponding experimental results from Brookhart and Rix are $\Delta E_{Me\rightarrow CO} = 15.4 < \Delta E_{Ac\rightarrow C_2H_4} = 16.6 < \Delta E_{Me\rightarrow C_2H_4} = 18.5$, with an error of ±0.1 kcal/mol. No value was reported for CO insertion into the Pd−Ac bond. The prediction of CO insertion into the Pd−Me bond as the lowest of the three experimentally measured insertions is in agreement with experiment. At this level of theory, the largest error, 2.3 kcal/mol, exists in the activation barrier for ethylene insertion into the Pd−Me bond. As discussed above, thermal effects reduce this error to 1.2 kcal/mol and larger basis sets reduce the error further to 0.9 kcal/mol. Even with these theoretical corrections, $\Delta E_{Me\rightarrow C_2H_4}$ and $\Delta E_{Ac\rightarrow C_2H_4}$ are reversed compared to the experiment.

The reactant, transition state, and insertion product in the CO insertion into the Pd−Me bond are approximately 10 kcal/mol lower in energy compared to those in the C_2H_4 insertion. The activation barrier for CO insertion is lower than the C_2H_4 activation barrier. On the other hand, in the insertion into the Pd−acyl bond, the CO insertion transition state **TS(6−8)** is 0.8 kcal/mol higher in energy and the barrier is 10.0 kcal/mol higher than that for the C_2H_4 insertion transition state **TS(7b−9)**. In addition, the CO insertion is endothermic and has no driving force. One can therefore conclude that the CO insertion into the Pd−Me bond is preferred over C_2H_4 insertion kinetically and thermodynamically, and for the Pd−acyl bond C_2H_4 insertion is again clearly favored over CO insertion kinetically and thermodynamically. Consequently, the reaction using the Pd catalyst should take place alternatingly. The rate-determining step in the copolymerization reaction using the Pd catalyst is ethylene insertion into the Pd−acyl bond, in agreement with experiment.

For Ni, the order of the activation energies (in kcal/mol) at the B3LYP/I level for the migratory insertion reactions is: $\Delta E_{Ac\rightarrow C_2H_4} = 6.3 < \Delta E_{Me\rightarrow CO} = 9.8 \approx \Delta E_{Me\rightarrow C_2H_4} = 9.9 < \Delta E_{Ac\rightarrow CO} = 24.9$. This order is clearly different from that for the Pd case, where the CO insertion into the metal−Me bond had the lowest activation barrier. As in the case of Pd, the reactant, transition state, and product in the CO insertion into the metal−Me bond are significantly lower in energy than those in the C_2H_4 insertion. Again as in the Pd case, the C_2H_4 insertion into the metal−acyl bond is easier than the CO insertion.

No significant kinetic preference for the carbonyl insertion compared to the olefin insertion into the metal−alkyl bond exists for Ni, in contrast to Pd. A thermodynamic preference for carbonyl insertion remains though, due to the larger binding energies of the carbonyl complex compared to the olefin complex. In the insertion into the metal−acyl bond, the olefin activation barrier is calculated to be 18.6 kcal/mol lower than the carbonyl barrier. In addition, as in Pd, no thermodynamic driving force exists for the CO insertion into the Ni−acyl bond. The rate-determining step in the copolymerization reaction using the Ni catalyst is the carbonyl insertion into the Ni−alkyl bond, in

Downloaded by CARLI CONSORTIUM on June 30, 2009
Published on December 24, 1996 on http://pubs.acs.org | doi: 10.1021/om960535u

contrast to Pd, for which the olefin insertion into the Pd−acyl bond is rate-determining. Another important difference between Ni and Pd is the significantly faster catalytic reaction for Ni. The rate-determining step for Pd has an activation barrier of 18.2 kcal/mol, compared to 9.9 kcal/mol for Ni at the B3LYP/I level.

Why are the activation barriers for Ni lower than for Pd? This can be rationalized by looking at the differences in driving force or exothermicity in the insertion steps. For instance, carbonyl insertion into the metal−methyl bond is 5.6 kcal/mol exothermic for Ni and is 2.0 kcal/mol endothermic for Pd, with a difference in driving force of 7.6 kcal/mol. The difference in the activation barriers for this insertion reaction is proportional to this, i.e., 5.2 kcal/mol. Using the same argument for the ethylene insertion into the metal−methyl bond, the driving force is 5.3 kcal/mol larger for Ni and at the same time the activation barrier is 6.3 kcal/mol lower for Ni. For ethylene insertion into the metal−acyl bond, the driving forces differ by 12.8 kcal/mol and the activation barriers by 11.9 kcal/mol. Larger driving forces are correlated with smaller activation barriers. The exothermicity of the insertion reaction is related to the difference in the stability between the metal−carbon bond formed in the insertion product and the CO or C_2H_4 π-complex. For Ni in comparison to Pd, σ-bonds are stronger than π-bonds. The reason for this is related to the larger difference for Ni in the size of the valence d orbitals and the valence s orbital. For Ni the d orbitals are more compact compared to those of Pd, thereby reducing the π-back-donation capacity. The relative strength of a σ-bond between the metal and the alkyl depends on the accepting rather than the back-donating capacity of the metal.

In general, why is the CO double insertion, the insertion of CO into the metal−acyl bond, by far the least favored among the four different insertion processes? This could be attributed to the weakest bond energy between the two CO groups. The bond dissociation energies from the experimental $\Delta H_{f,298K,g}$ values for CH_3-CH_3, CH_3-CHO, and CHO−CHO are 89.7, 85.1, and 72.0 kcal/mol;[25] the −CO−CO− bond formed in the double insertion is 13−18 kcal/mol weaker than the $-CH_2-CH_2-$ and $-CH_2-CO-$ bonds formed in the other insertion processes. This is strongly reflected in the calculated energy of reaction for this process (the only strongly endothermic insertion step for either Ni or Pd) as well as in the high activation barrier height.

V. Conclusions

We conclude the present paper with a brief summary of our predictions.

(1) The copolymerization reaction is predicted to be significantly faster using the Ni-based catalyst compared to the Pd-based catalyst. The rate-determining step for the Ni catalyst is CO insertion into the metal−alkyl bond.

(2) The selectivity for completely alternating polymerization is predicted to be smaller for Ni-based catalysts compared with the Pd-based catalyst.

Acknowledgment. We are grateful to Mr. Qiang Cui for the ECP analytical second-derivative program and Dr. Jamal Musaev for his help and numerous and discussions. The use of the Emerson Center computing facilities is acknowledged. The present research was in part supported by Grants CHE-9409020 and CHE-9627775 from the National Science Foundation. M.S. acknowledges a fellowship from the Swedish Natural Science Research Council.

OM960535U

(25) NIST Standard Reference Database No. 69 (1996).

Downloaded by CARLI CONSORTIUM on June 30, 2009
Published on December 24, 1996 on http://pubs.acs.org | doi: 10.1021/om960535u